

Diffusion Meets DAgger: Supercharging Eye-in-hand Imitation Learning

Xiaoyu Zhang* Matthew Chang* Pranav Kumar Saurabh Gupta
*project co-leads

University of Illinois at Urbana-Champaign
{zhang401,mc48,pranav9,saurabhg}@illinois.edu
<https://sites.google.com/view/diffusion-meets-dagger>

arXiv:2402.17768v1 [cs.RO] 27 Feb 2024

Abstract—A common failure mode for policies trained with imitation is compounding execution errors at test time. When the learned policy encounters states that were not present in the expert demonstrations, the policy fails, leading to degenerate behavior. The Dataset Aggregation, or DAgger approach to this problem simply collects more data to cover these failure states. However, in practice, this is often prohibitively expensive. In this work, we propose Diffusion Meets DAgger (DMD), a method to reap the benefits of DAgger without the cost for eye-in-hand imitation learning problems. Instead of *collecting* new samples to cover out-of-distribution states, DMD uses recent advances in diffusion models to *create* these samples. This leads to robust performance from few demonstrations. In experiments conducted for non-prehensile pushing on a Franka Research 3, we show that DMD can achieve a success rate of 80% with as few as 8 expert demonstrations, where behavior cloning reaches only 20%. DMD also outperform competing NeRF-based augmentation schemes by 50%.

I. INTRODUCTION

Imitation learning is an effective way to train robots. However, even when testing policies in environments similar to those used for training, imitation learning suffers from the well-known *Compounding Execution Errors problem*: small errors made by the learned policy lead the robot to out-of-distribution states causing the learner to make even bigger errors (compounding errors) [56].

One solution to this problem is via manual collection of expert-labeled data on states visited by the learner, a strategy popularly known as Dataset Aggregation or DAgger [56]. In theory, this solution works. However, putting it into practice is challenging from a practical stand point: driving a robot that doesn't obey your commands is difficult. Many alternatives have been proposed, *e.g.* [35, 36], but they all require collecting more expert data. In this paper, we pursue an alternate paradigm: *automatically generating observations and action labels for out-of-distribution states*. By replacing data collection with data creation, we improve the sample efficiency of imitation learning. In fact, data creation was Pomerleau's original solution to this problem [51]. We revisit, improve, and automate his solution from 30 years ago using modern data-driven image generation methods. We do this for imitation learning problems in context of eye-in-hand setups (*i.e.* setups where images come from a camera mounted on the robot hand) that are increasingly becoming more popular [64, 77, 84].

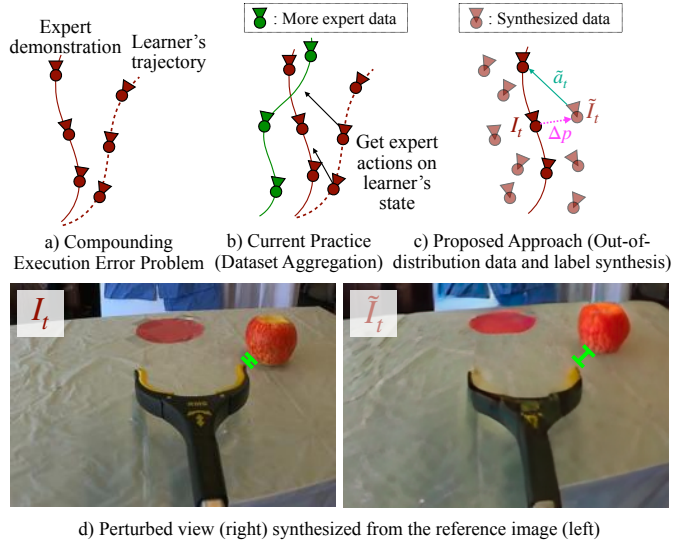


Fig. 1: Eye-in-hand Imitation learning with DMD: A common failure mode in an imitation learning setting is the problem of poor generalization due to compounding execution errors at test time as shown in (a). This can be solved by collecting more expert data to cover these off-trajectory states as shown in (b) however, this is an expensive process. Our proposed approach is to *synthesize* data instead of *collecting* it (c). **Magenta** arrow represents small perturbation (Δp) to the trajectory. **Cyan** arrow represents label (\tilde{a}_t) for this out-of-distribution observation. We use a state-of-the-art diffusion model to take images I_t from expert demonstrations (d, left) and generate realistic off-trajectory images \tilde{I}_t (d, right). Note the distance between the grabber and the apple denoted by the green line. This synthetic data augments expert demonstrations for policy learning, leading to more robust policies.

In more detail: given a behavior cloning trajectory, τ collected from an expert operating the system, we design generative models to synthesize off-distribution states and corresponding action labels. For example, for the object pushing application in Figure 1, this would correspond to generating off-center views of the object from the good expert trajectory τ . Specifically, we learn a function $f(I_t, \Delta p)$ that synthesizes the observation \tilde{I}_t at a small perturbation Δp to the trajectory at time step t . Knowledge of this Δp lets us compute the ground truth action label \tilde{a}_t for this out-of-distribution observation. We augment the expert demonstration τ with multiple off-distribution samples (\tilde{I}_t, \tilde{a}_t) along the trajectory. Access to out-of-distribution states and action labels for how

to recover from them improves the performance of the task policy.

In this paper, we develop and evaluate this idea in context of eye-in-hand manipulation policies in the real world. While the idea is intuitive, a number of nuances have to be dealt with carefully to get it to work. As we have access to the entire trajectory, the natural choice is to adopt NeRFs [48, 85] to realize the function f . While NeRFs work very well for view synthesis in computer vision, we found that they don't work well for the synthesis task at hand because of the inevitable deformations in the scene as the gripper manipulates the objects. We thus switched to using diffusion models for this synthesis task. This led to good image synthesis even in situations where the scene deformed over the course of manipulation. Computing action labels for these samples presented yet another challenge (Figure 6). The labels should align with making progress towards the goal. We thus investigated different schemes for sampling Δp 's and computing action labels \tilde{a}_t .

This paper presents experiments that evaluate the aforementioned design choices to develop a data creation framework to supercharge eye-in-hand imitation learning. Experiments on a physical platform demonstrate the effectiveness of our proposed framework over baseline data augmentation techniques. On a non-prehensile pushing on a Franka Research 3, we show that DMD can achieve a success rate of 80% with as few as 8 expert demonstrations, where behavior cloning reaches only 20%. We also outperform a recently proposed augmentation scheme based on NeRFs [85] by 50%.

II. RELATED WORK

A. Imitation Learning

Behavior cloning (BC), or training models to mimic expert behavior, has been a popular strategy to train robots over the last many decades [50, 51, 58] and has seen a recent resurgence in interest [28, 86]. Ross et al. [56] theoretically and empirically demonstrate the compounding execution error problem (small errors in the learner's predictions steer the agent into out-of-distribution states causing the learner to make even bigger errors) and propose a Dataset Aggregation (DAgger) strategy to mitigate it. Over the years, researchers have sought to improve the basic BC and DAgger recipe in several ways [4, 25]. [17, 62, 64, 77, 84] devise ways to ease and scale-up expert data collection, while [83] design ways to collect demonstrations in virtual reality. [35, 36] devise ways to simplify DAgger data collection. [14, 61] model the multiple modes in expert demonstrations, while [49] employ a non-parameteric approach. Researchers have also shown the effectiveness of pre-trained representations for imitation learning [49, 74]. [12, 46, 81, 85] employ image and view synthesis models to synthetically augment data. Complementary to our work, [12, 46, 81] focus on generalization across objects via *semantic* data augmentation by adding, deleting and editing objects in the scene.

[16, 31, 32, 85] pursue synthetic data augmentation to address the compounding execution error problem. [16, 31]

conduct these augmentation in low dimensional state spaces. Ke et al. [32] leverage local continuity in the environment dynamics to generate corrective labels for low-dimensional state spaces and LiDAR observations in simulation. Closest to our work, Zhou et al. [85]'s SPARTN model train NeRF's on demonstration data to synthesize out-of-distribution views. NeRF assumes a static scene. Thus, SPARTN can't reliably synthesize images when the scene undergoes deformation upon interaction of the robot with the environment. Our use of diffusion models to synthesize images gets around this issue and experimental comparison to SPARTN demonstrate the effectiveness of our design choice.

B. Image and View Synthesis Models

Recent years have witnessed large progress in image generation [18, 24, 54, 63, 65]. This has led to a number of applications: text-conditioned image generation [5, 20, 52, 54, 57, 82], image and video inpainting [9, 44, 47], image to image translation [27] and generation of novel views for objects and scenes from one or a few images [34, 42, 69, 72, 80]. While diffusion models have proven effective at image synthesis tasks, Neural Radiance Fields (NeRFs) [48] excel at view interpolation tasks. Given multiple (20 – 100) images of a static scene, vanilla NeRFs can effectively interpolate among the views to generate photo-realistic renders. Researchers have pursued NeRF extensions that enable view synthesis from few images [7, 19, 75, 79] and even model deforming scenes [8, 66]. In general, NeRFs are more effective at interpolation problems, while diffusion models excel at problems involving extrapolation (*e.g.* synthesizing content not seen at all) or where exactly modeling changes in 3D is hard (*e.g.* deforming scenes). As our work involves speculating how the scene would look if the gripper were at a different location, we adopt a diffusion based methods. We show comparison against a NeRF based method as well.

C. Diffusion Models and Neural Fields for Robot Learning

Effective generative models and neural field based representations have been used in robotics in other ways than for data augmentation. Researchers have used diffusion models for representing policies [1, 13, 37, 38, 71], generating goals or subgoals [6, 10, 30], offline reinforcement learning [3, 43, 71], planning [29, 40, 41, 73], behaviorally diverse policy generation [23], and predicting affordances [76]. Additionally, they have been used to generate samples with high reward [26] and skill acquisition from task or play data [11]. Neural fields have been used to represent scenes for manipulation [39, 70] and navigation [2].

III. APPROACH

A. Overview

Given task data \mathbf{D} , imitation learning learns a task policy π . The task data takes the form of a collection of trajectories τ_i , where each trajectory in turn is a collection of image action pairs, (I_t, a_t) . π is trained using supervised learning to regress action a_t from images I_t over the task data \mathbf{D} . For

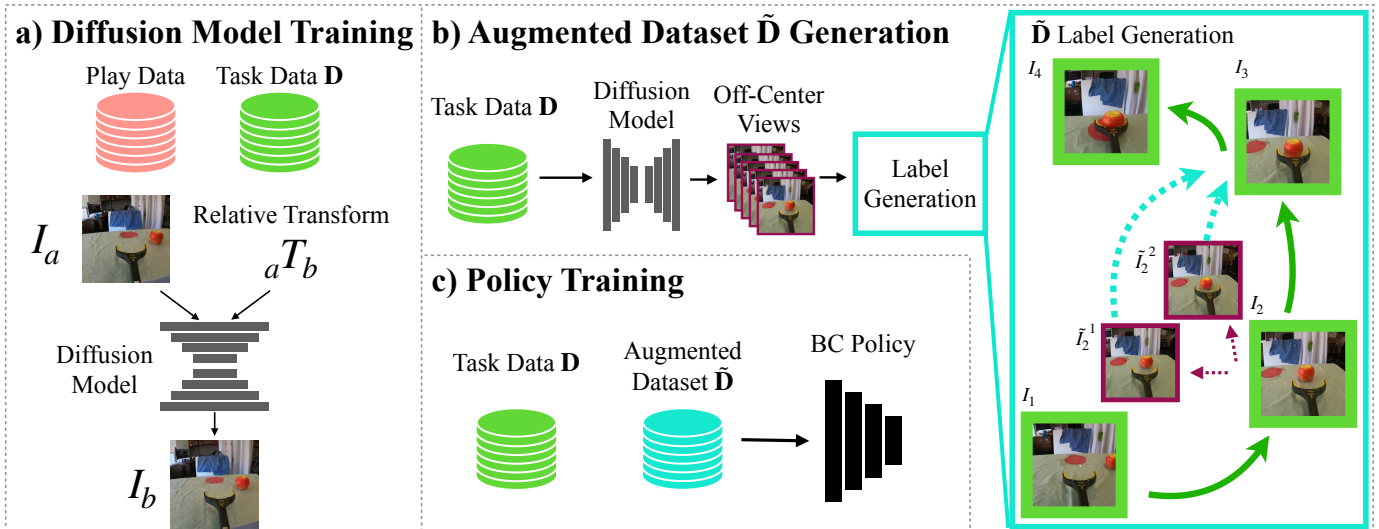


Fig. 2: DMD System Overview: Our system operates in three stages. a) A diffusion model is trained, using task and play data, that can synthesize novel views of a scene relative to a given image. b) This diffusion model is used to generate an augmenting dataset that contains off-trajectory views ($\tilde{I}_1^1, \tilde{I}_2^2$) from expert demonstrations. Labels for these views (cyan arrows) are constructed such that off-trajectory views will still converge towards task success (right). Images with a green border are from trajectories in the original task dataset. Purple-outlined images are diffusion-generated augmenting samples. c) The original task data and augmenting dataset are combined for policy learning.

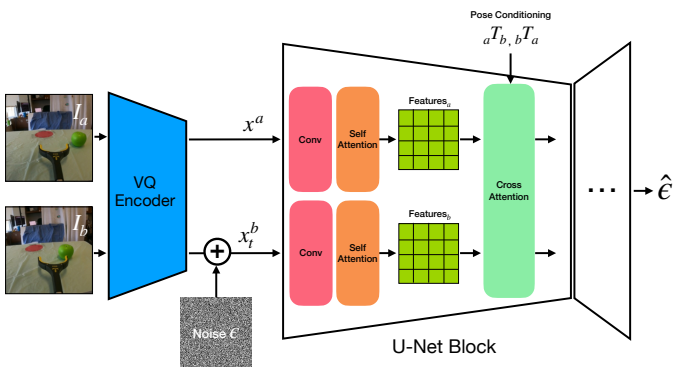


Fig. 3: DMD Architecture: We use the architecture introduced in [80], a U-Net diffusion model with blocks composed of convolution, self-attention, and cross attention layers. The conditioning image I_a , and noised target image I_b are processed in parallel except at cross-attention layers. The pose conditioning information is injected at cross-attention layers.

the non-prehensile manipulation of objects using an eye-in-hand cameras considered in this paper, images I_t correspond to views from the eye-in-hand camera as input, and the actions a_t are the relative end-effector poses between consecutive time steps.

When trained with few demonstrations, π exhibits poor generalization performance. To address poor generalization, our approach generates an augmented dataset $\tilde{\mathbf{D}}$ and trains the policy jointly on $\tilde{\mathbf{D}} \cup \mathbf{D}$. Augmented samples are specifically generated to be out-of-distribution from \mathbf{D} and thus aid the policy’s generalization capabilities. $\tilde{\mathbf{D}}$ is generated through a conditional diffusion model f that generates a Δp perturbed view \tilde{I} of an image I_t from a given trajectory τ : $\tilde{I} = f(I_t, \Delta p)$. We use the action labels in the trajectory τ to compute the action label \tilde{a} for this perturbed view. We describe the design of the conditional diffusion model in Section III-B

and detail the augmenting image sampling and action labels computation procedure in Section III-C.

B. Diffusion Model for Synthesizing Δp Perturbed Views

The function $f(I, \Delta p)$ is realized using a conditional diffusion model that is pretrained on large Internet-scale data. Specifically, we adopt the recent work from Yu et al. [80] and finetune it on data from \mathbf{D} . The model produces image I_b by conditioning on a reference image I_a taken by camera a and a transformation matrix ${}_aT_b$ that maps points in camera b ’s frame to camera a ’s frame. By representing the desired Δp as the transformation between two cameras (${}_aT_b = \Delta p$), and using images from \mathbf{D} as the reference images ($I_a \sim \mathbf{D}$), the learned diffusion model can generate the desired perturbed views for augmenting policy learning.

1) *Model Architecture:* A diffusion model can be thought of as an iterative denoiser: given a noisy image x_t , diffusion timestep t , it is trained to predict the noise ϵ added to the image.

$$\mathcal{L} = \|\epsilon - \epsilon_\theta(x_t, t)\|_2^2$$

It is typically realized via a U-Net [55]. Our application requires *conditional image generation* where the conditions are source image I_a and transformation ${}_aT_b$. Thus, by using I_b as the diffusion target, and conditioning on I_a and ${}_aT_b$, the model ϵ_θ learns to denoise new views of the scene in I_a based on the transformation ${}_aT_b$. Finally, rather than directly denoising in the high-resolution pixel space, the denoising is done in the latent space of a VQ-GAN autoencoder, E [15, 53]. This gives the final training objective of:

$$\mathcal{L} = \|\epsilon - \epsilon_\theta(x_t^b, E(I_a), {}_aT_b, t)\| \quad \text{where } x_0^b = E(I_b).$$

Following [80], the pose conditioning information ${}_aT_b$ is injected into the U-Net via cross-attention as shown in Figure 3.

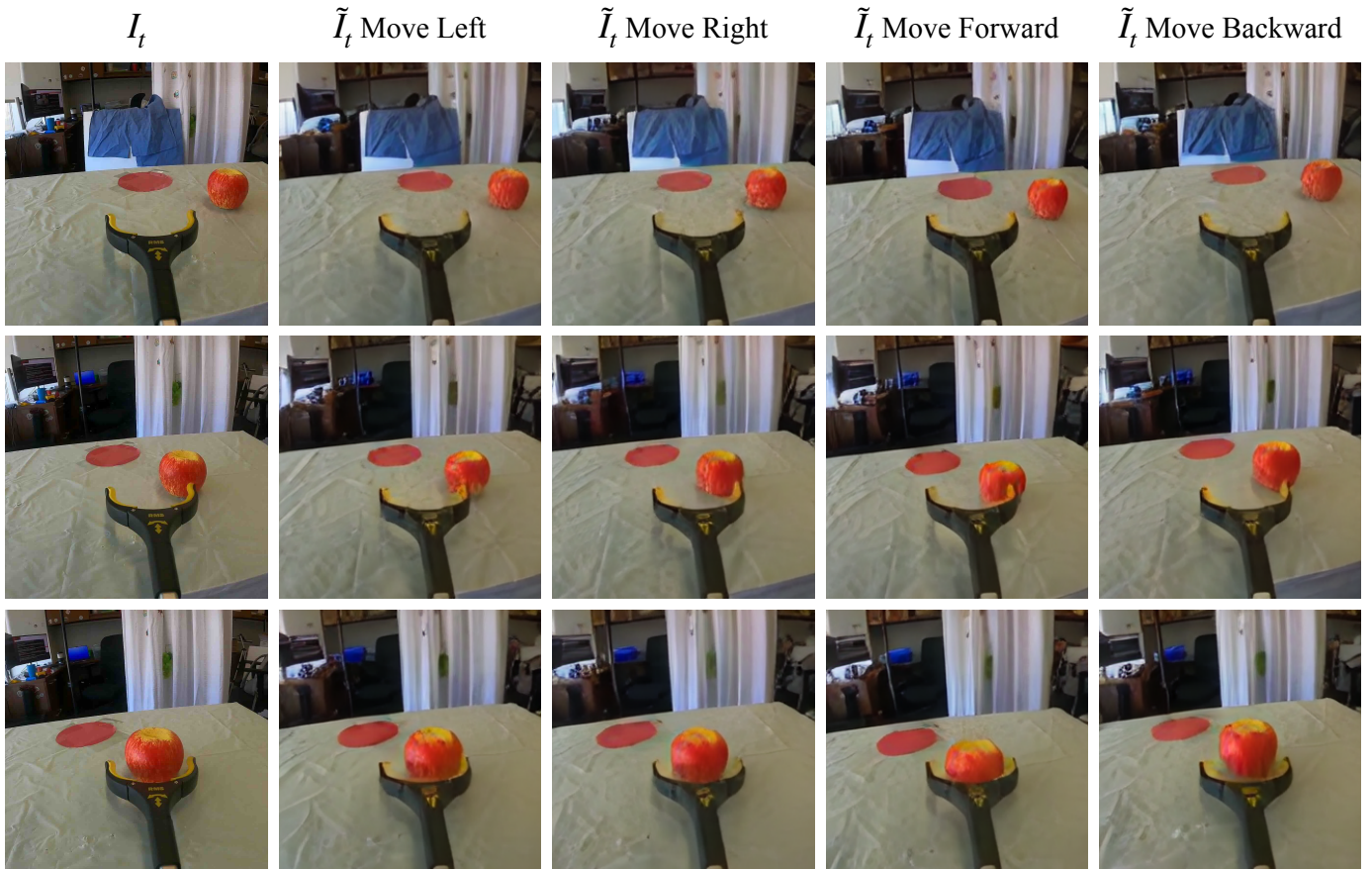


Fig. 4: Visualization of perturbed images generated by diffusion model for augmenting policy learning. In each row, we show \tilde{I}_t generated from I_t through different camera translations.

2) *Model Training*: Training the model requires access to triples: $(I_a, I_b, {}_aT_b)$. We process data from \mathbf{D} to generate these triples. Let each trajectory consist of images I_1, \dots, I_N . We use the structure from motion [21, 68] implementation from the COLMAP library [59, 60] to extract poses for the images in the trajectory τ . This associates each image I_t in the trajectory with the (arbitrary) world frame ${}_tT_w$. We can then compute relative pose between arbitrary images I_a and I_b from a trajectory via ${}_aT_b = {}_aT_w T_b$. We sample random pair of images from the trajectory to produce triples $(I_a, I_b, {}_aT_b)$ that are used to train the model ϵ_θ . COLMAP also outputs the camera intrinsics necessary for training the model. Since COLMAP reconstruction is only correct up to a scale factor, we normalize translations by the largest displacement between adjacent frames per trajectory.

As \mathbf{D} contains much less data than is typically required to train a diffusion models from scratch, we finetune the model from Yu et al. [80]. We find that finetuning with as few as 24 trajectories leads to realistic novel view synthesis for our task as shown in Figure 4. We only finetune the diffusion model weights and use the pre-trained VQ-GAN codebooks. We experiment with different datasets for finetuning this diffusion model: task data from \mathbf{D} , play data [45, 78] collected in our setup, and their combinations.

C. Generating Out-of-Distribution Images and Labels

1) *Sampling Out-of-distribution Images*: We generate out of distribution views for images in the task dataset \mathbf{D} . Δp 's are sampled as follows. For an image I_t from trajectory τ , we sample vectors in a random direction, with magnitude drawn uniformly from $[0.2s, s]$, where s is the largest displacement between adjacent frames in τ . Δp simply corresponds to translation along this randomly chosen vector. We constrain these samples to not be too aligned with the actual action.

2) *Labeling Generated Images*: For each image $\tilde{I}_t = f(I_t, \Delta p)$ generated from an original image I_t , we use I_{t+k} as the target for generating the action label. The action label for \tilde{I}_t is simply the action that would convey the agent from the pose depicted in \tilde{I}_t to the pose in I_{t+k} .

From COLMAP, we obtain camera pose information ${}_tT_w$ for time step t and ${}_{t+k}T_w$ for time step $t+k$. The synthesized view \tilde{I}_t can be treated as an image taken by a virtual camera whose pose is represented as ${}_tT_{\tilde{t}}$. The diffusion model synthesizes perturbed view conditioned on I_t and ${}_tT_{\tilde{t}}$, or $\tilde{I}_t = f(I_t, {}_tT_{\tilde{t}})$ (Section III-B). The action label \tilde{a}_t for \tilde{I}_t is then computed as $\tilde{a}_t = {}_{\tilde{t}}T_{t+k} = {}_{\tilde{t}}T_t {}_tT_w ({}_{t+k}T_w)^{-1}$. Examples of $(\tilde{I}_t, \tilde{a}_t)$ are shown in Figure 5.

One might wonder why we don't just use $k = 1$? As the scale of each trajectory is different, the diffusion model

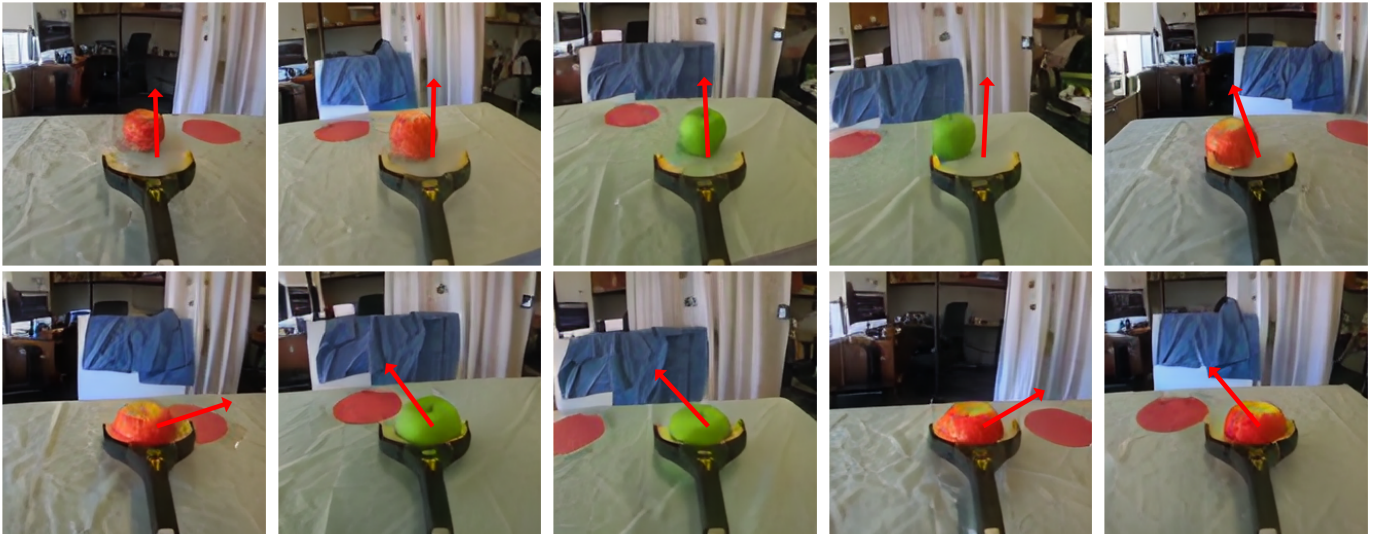


Fig. 5: Training Examples from the Diffusion Model: We visualize generated examples, \tilde{I} , used to train our policies along with the computed action label (the arrow is a projection of the 3D action into the 2D image plane: the arrow pointing up means move the gripper forward, pointing to the right means move it right). We show augmentations generated by our diffusion model for at different stages of the task. The first row shows augmentations from images where the gripper approaches the apple, while the second row shows augmentations from images where the gripper moves the apple towards the goal location.

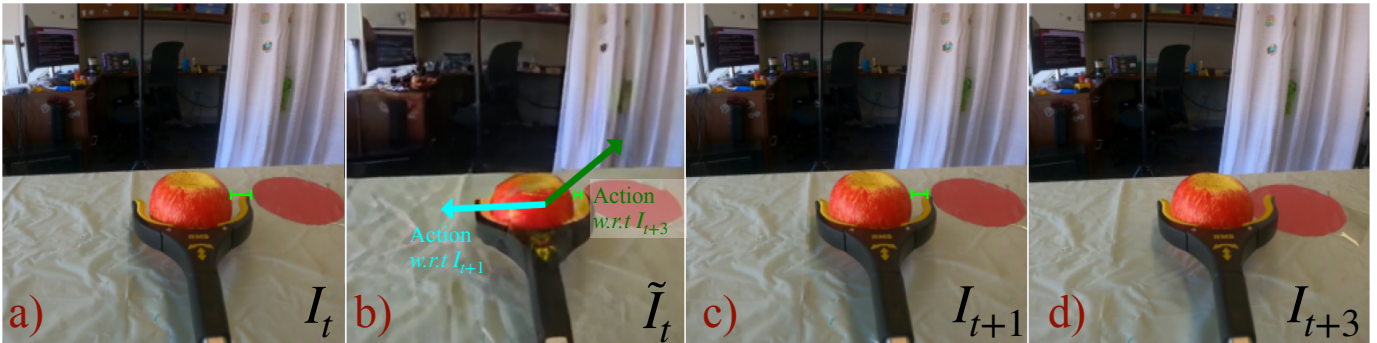


Fig. 6: The overshooting problem: Under certain conditions, the inferred action for \tilde{I}_t may direct the agent away from task success. We refer to this as the overshooting problem. At time step $t + 1$, the view I_{t+1} in (c) has moved to the right from I_t in (a). However, the synthesized sample \tilde{I} (b) has moved even further to the right than I_{t+1} . In (b), Cyan arrow represents action label for \tilde{I}_t computed using I_{t+1} as the target; green arrow represents action label computed using I_{t+3} as the target. Since \tilde{I}_t has “overshot” I_{t+1} , an action taken with I_{t+1} as the next intended target moves backward, away from the goal. Computing the action with respect to a farther image, say I_{t+3} in (d), does not have this issue.

learns the distribution of scales over \mathbf{D} . Depending on the scale of the COLMAP reconstruction, this causes the generated samples to move more than 1 unit for some trajectories. When using $k = 1$, some generated samples move past the target image I_{t+1} (as described in Figure 6). This causes conflicting supervision, as the computed action does not make progress toward completing the task. Using a large k guards against this, leading to stronger performance downstream, as our experiments verify (Section IV-C2).

IV. EXPERIMENTS

A. Experiment Setup

1) *Task, Observation Space, Action Space:* We use the non-prehensile pushing task from VIME [77] as a benchmark task. The task is to push the target object to a target location marked by a red circle and requires both reaching and pushing the object. Following Young et al. [77], we use a grabber as the

robot end-effector as shown in Figure 7. This allows for easy collection of expert demonstrations using a GoPro mounted on a Grabber. Due to the difference in joint limits between the XArm (used by VIME) and the Franka Research 3 robot, we redesign the attachment between the grabber and the robot flange. In this way, the robot can execute planar push in the typical top-down configuration, extending the workspace to a wider range of the table. The comparison is shown in Figure 7. Observations come from the eye-in-hand GoPro camera. We use the action space used in VIME’s [77] publicly available code: relative 3D translations of the end-effector.

2) *Task and Play Data:* We collect task and play data trajectories using a GoPro mounted on a Grabber. For task data, an expert pushes the object to a target location. For play data, we move the grabber around the apple and push it in many different directions. Through this procedure, we only get image sequences. We use structure from motion [21, 68]

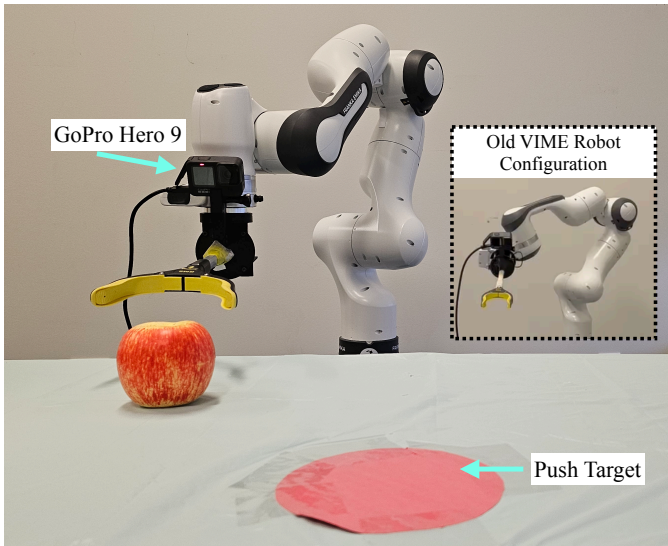


Fig. 7: Robotic Platform for Online Testing: We conduct our experiments on a Franka Research 3 robot with a wrist-mounted GoPro Hero 9. In the depicted configuration, the task is to push the apple onto the red circle. Since VIME’s [77] action space is relative 3D translations, we modified its grabber mount on the robot, allowing the robot to move without reaching joint limits while preserving the original rotation of the end-effector.

to extract camera poses tT_w for images in the collected sequences. Action a_t is computed as the relative translation between I_{t+1} and I_t in I_t ’s camera frame. Since COLMAP only gives reconstructions upto an unknown scale factor, following [77] we normalize the action to unit length and interpret it as just a direction. Since the final robot action space is 3D translation, we avoid rotating the grabber during both type of data collection; however, slight rotation of the grabber still exists in expert demonstrations.

3) *Policy Architecture and Execution:* We adopt the architecture for the task policy π from VIME [77] but replace the AlexNet [33] backbone with an ImageNet pre-trained ResNet-18 backbone [22]. The policy consists of the ResNet backbone followed by 3 MLPs that predict the action. This task policy accepts a center cropped image from the GoPro camera and outputs the direction in which the camera should move. The policy is trained by L1 regression to the (unit length) actions using the Adam optimizer with a learning rate of $1e-4$. Actions are executed on the robot by commanding the robot to go 1cm in the predicted direction.

4) *Comparisons:* We use behavior cloning on the expert data as done in past work [77], as the baseline. We refer to this as BC. We also compare to SPARTN [85] and evaluate the various design choices. Since there is no publicly available code from SPARTN, we replicate their procedure using NerfStudio [67].

B. Visual Comparison of Generated Images

We start by assessing the visual quality of samples generated by the diffusion model in DMD. Figure 4 and Figure 5 shows sample images generated by our diffusion model. The model is able to faithfully generate images where the camera is moved

left / right and front / back with minimal artifacts.

We also compare the visual quality of our generated images to those generated using the NeRF based approach from SPARTN [85]. The moving gripper in the scene breaks the static scene assumption made by NeRF. Thus, [85] mask out the gripper before training the NeRF. While this works for the pre-grasp trajectory that Zhou et al. [85] seek to imitate, this strategy fails when the gripper actually manipulates the scene, as in our task. Thus, we investigate different masking schemes: a) no masking, b) masking a larger region around the gripper, c) masking just the gripper; and show visualizations in Figure 8. No masking leads to the worst results as expected. Masking just the grabber fixes the grabber, but causes the object being manipulated to blur out. Masking a larger region around the grabber fixes the blurring but also eliminates the object being manipulated. In contrast, images synthesized using our diffusion model move the camera as desired without creating any artifacts.

C. Offline Validation

We collected 74 expert demonstrations in total for the apple pushing task. We use 24, 23, and 27 trajectories for train, validation, and test, respectively. We use vanilla behavior cloning on the expert data as the baseline as done in past work [77]. Our offline validation involves evaluating the policy’s predictions on the test set. While the test set samples doesn’t contain examples of going off the distribution, it does measure generalization to some extent by evaluating the policy on states outside of the training set. For the error metric, we use the median angle between the predicted and the ground truth translation.

We conduct offline validation to compare with other data augmentation schemes and select the value of k to mitigate the over-shooting problem. Online experiments in Section IV-D test the success rate of the policy.

TABLE I: Comparisons between diffusion-generated augmented dataset and standard augmentation schemes. The table shows median angle error (in radians) between predicted and ground-truth translations. Adding $\bar{\mathbf{D}}$ generated by diffusion models improve performance on top of other augmentation techniques.

| Methods | BC | DMD |
|------------------------|-------|--------------|
| No Aug | 0.376 | 0.349 |
| w/ Color jitter | 0.381 | 0.350 |
| w/ Flip | 0.356 | 0.338 |
| w/ Color jitter & Flip | 0.355 | 0.328 |

1) Comparison with other data augmentation schemes:

We want to understand the effectiveness of augmenting with diffusion-generated images compared to augmenting with standard techniques, such as color jitter and horizontal flip. Table I shows that augmentation, in general, improves performance, and augmenting with out-of-distribution images leads to larger improvement compared to standard techniques. Comparing the two columns, we see that adding diffusion-generated images improve performance in all settings.

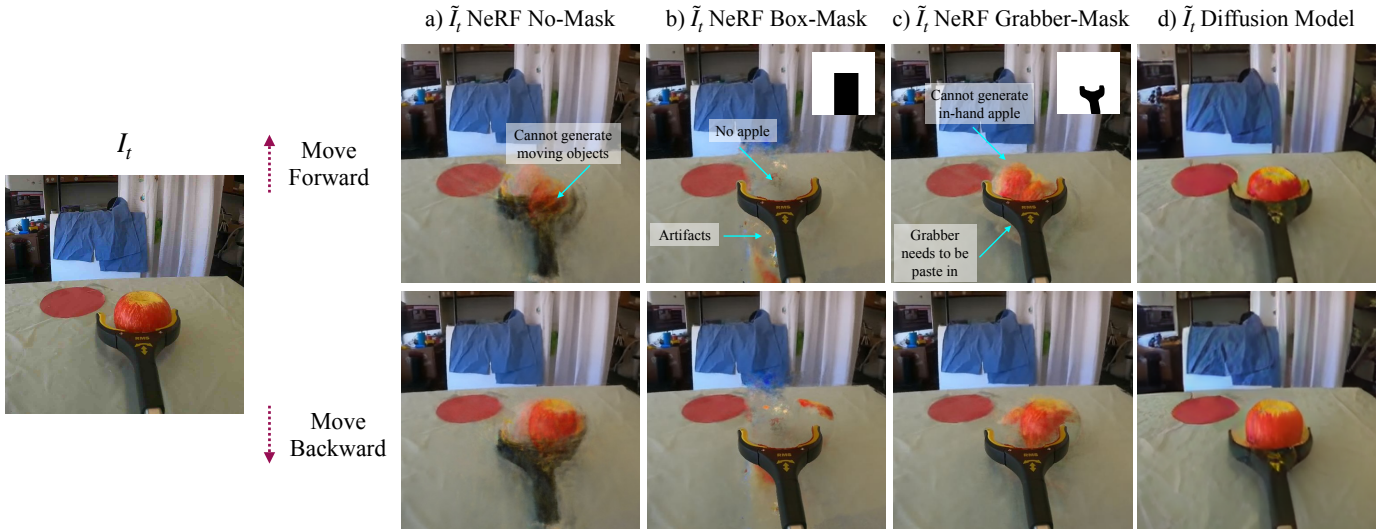


Fig. 8: Diffusion vs NeRF Here we visualize perturbed samples generated using DMD and NeRF baselines with different masking strategies. The top row shows images generated corresponding to a forward movement relative to I_t , and the bottom row for a backward movement. When using a NeRF with no masking (a), the reconstructions of the gripper and apple are degenerate, as they violate the static scene assumption in NeRFs. With a box-mask (b), the apple is occluded by the mask, and consequently, missing from the reconstruction. Even with a mask around the end-effector (Grabber-Mask), there are major artifacts in reconstructing the apple (c). With ours (Diffusion Model), the model faithfully reconstructs the gripper and apple (d).

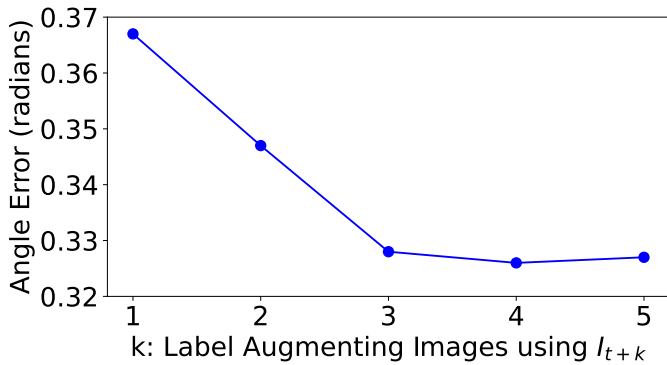


Fig. 9: Effect of using different future frames for labeling augmenting images on translation prediction: to overcome the overshooting problem described in Figure 6, we experiment with different future frame I_{t+k} for labeling the diffusion model generated images. Error decreases as k increases and plateaus around $k = 3$. Therefore, we use frame I_{t+3} for labeling \tilde{I}_t

2) *Overshooting problem, what frame to use?:* In order to mitigate the overshooting problem, we use image $I_{t+k}, k > 1$ to label the augmenting image instead of I_{t+1} . We evaluate policies trained with labels produced from different k 's, and show the results in Figure 9. We find that labeling with I_{t+1} 's pose works worse than labeling with pose for I_{t+3} and beyond. As the curve plateaus beyond $k = 3$ and using larger k leads to the exclusion of the last $k - 1$ frames in each trajectory, we use $k = 3$ for our online experiments.

D. Online Validation

Our online experiments measure the success rate at the non-prehensile pushing task. We conduct 10 trials per method and randomize the apple start location between trials. To prevent human biases, we choose the apple start location before sampling the method to run next. Execution trajectories

TABLE II: Online Robot Experiment Results. We conduct 5 experiments: 10 trials per method and randomize the apple start locations between trials.

| Method | Success Rate | Method | Success Rate |
|--------|--------------|--------|--------------|
| BC | 30% | SPARTN | 50% |
| DMD | 100% | DMD | 100% |

a) DMD vs. Behavior Cloning b) DMD vs. SPARTN

| Method | 16 Demonstrations | 8 Demonstrations |
|--------|-------------------|------------------|
| BC | 50% | 20% |
| DMD | 90% | 80% |

c) DMD with Few Demonstrations

| Method | Success Rate | Method | Success Rate |
|-------------|--------------|--------|--------------|
| Task | 80% | BC | 80% |
| Task + Play | 100% | DMD | 90% |

d) Utility of Play Data for Training Diffusion Model e) Scaling to Other Objects

can be found on the project website.

1) *DMD vs. Behavior Cloning:* We take the best model for BC and DMD from Table I and evaluate them on the robot. We find the vanilla BC model to get a 30% success rate while DMD achieves 100% (Table II a). This significant difference shows that minor error at each step can accumulate and result in task failure.

2) *DMD with Few Demonstrations:* Motivated by the 100% performance of DMD with 24 demonstrations, we ask how low can the number of demonstrations be? We consider 2 low data settings with 8 and 16 demonstrations. For these settings, the diffusion model is trained with only play data. Success rate for these two models on the robot is shown in Table II c. Once again DMD outperforms BC and achieves 80% success even

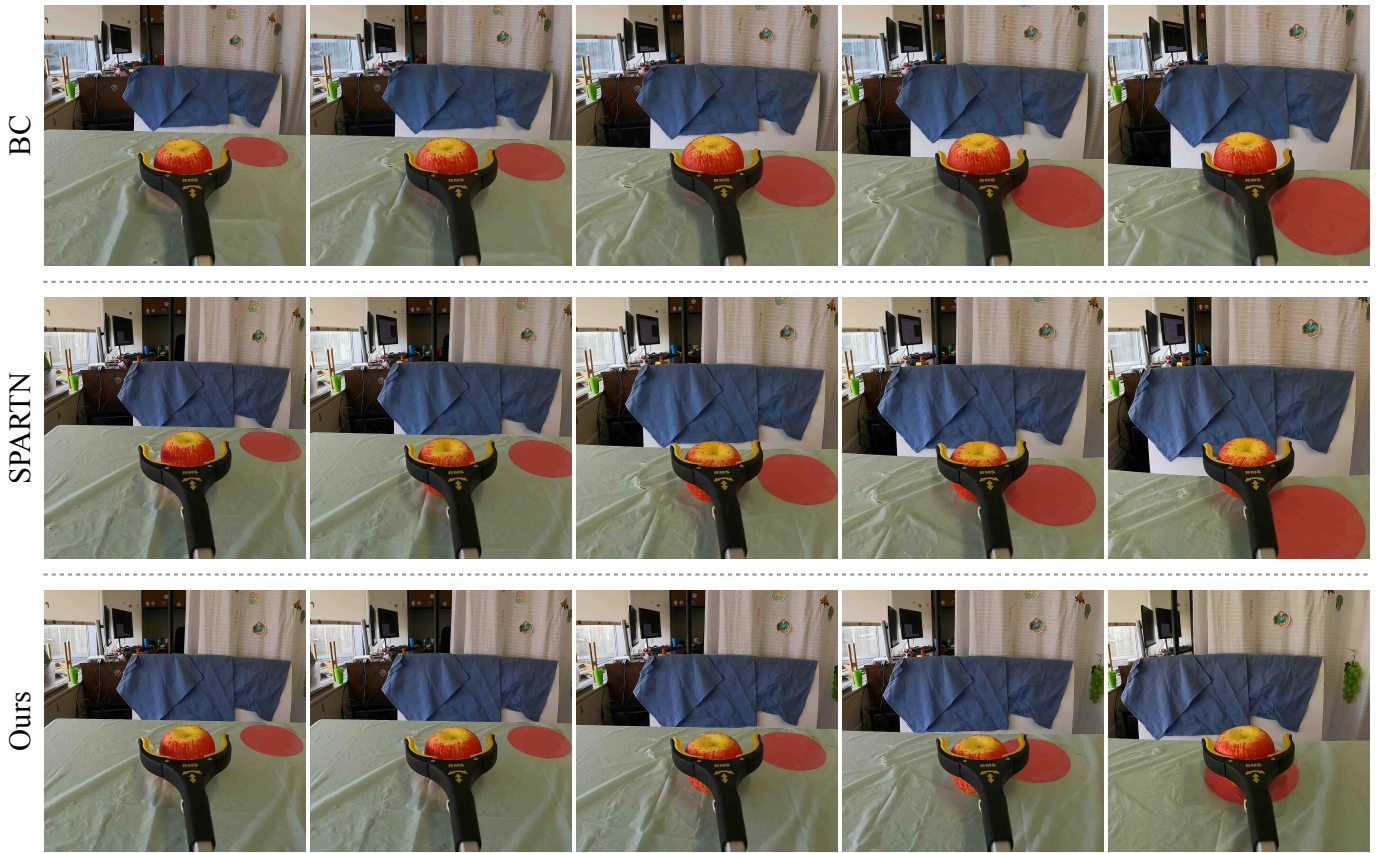


Fig. 10: Comparison of different methods on staying on course. We show the trajectories executed by BC, SPARTN [85], and DMD over several steps towards the target. Unlike BC and SPARTN, which gradually deviate from the intended path, DMD maintain its course towards the right and reach the target successfully. See project website for more execution videos.

when trained with only 8 demonstrations.

3) *DMD vs. SPARTN [85]*: Following up on the visual comparison of the quality of the augmenting samples from Section IV-B, we conduct a head-to-head comparison against SPARTN on the real robot. SPARTN achieves a success rate of 50% vs. DMD succeeds 100% of the time (Table II b). In Figure 10, we show that while SPARTN diverges from the expert course and pushes the apple off the table, DMD brings the apple to the target successfully.

4) *Utility of Play Data for Training Diffusion Model*: We also experimentally validate what the choice of the dataset necessary for training an effective diffusion model for view synthesis. We repeat the experiment with 24 demos but vary the diffusion model that generated the augmenting samples. Using the diffusion model trained on just task data lead to an 80% success rate vs. 100% success rate with the diffusion model trained on a combination of task and play data (Table II d). Thus, while just training the diffusion model on task data is effective (a nice result in practice), performance can be boosted further by training the diffusion model on play data.

5) *Scaling to Other Objects*: We conduct an experiment on another object, a cup. The BC baseline achieves a success rate of 80% vs DMD achieves a success rate of 90% (Table II e).

V. DISCUSSION

DMD was designed to improve the sample efficiency of eye-in-hand imitation learning. Compared to traditional behavior cloning, DMD shows significant improvement in experiments involving non-prehensile pushing across 2 objects. Remarkably, DMD provides effective augmenting strategies using generated images and enabled learned policies to achieve 80% success rate from as few as 8 demonstrations. DMD not only performs better than conventional augmentation schemes used in robotics but also shows improved metrics when combined with them.

Our experiments revealed the benefits of the different parts of DMD over past approaches. The use of diffusion models to synthesize images allows DMD to generate augmenting images for manipulation tasks that involve non-static scene. Prior work [85] used NeRFs instead of diffusion models, restricting generation to samples from pre-grasp part of the trajectories. We showcase the advantages of diffusion models over NeRFs through qualitative results in Figure 8 and real robot experiments in Section IV-D3. We also tested which type of data: task data, play data, or a combination of both, should be used for training the diffusion model. We found all versions to outperform behavior cloning. This suggests two

practically useful results. First, DMD can directly be used to improve a task policy without the need to collect any additional data, *i.e.* the task data itself can be used to finetune a novel-view synthesis diffusion model to augment the task dataset to improve performance. Second we can benefit from play data, which maybe simpler to collect than task data. To foster replication and future work, we will make code, data, and models publicly available.

ACKNOWLEDGMENTS

We give special thanks to Kevin Zhang for 3D printing the attachment for us. This material is based upon work supported by the USDA/NSF AIFARMS National AI Institute (USDA #2020-67021-32799) and NSF (IIS-2007035).

REFERENCES

- [1] Suzan Ece Ada, Erhan Oztop, and Emre Ugur. Diffusion policies for out-of-distribution generalization in offline reinforcement learning. *arXiv preprint arXiv:2307.04726*, 2023.
- [2] Michal Adamkiewicz, Timothy Chen, Adam Caccavale, Rachel Gardner, Preston Culbertson, Jeannette Bohg, and Mac Schwager. Vision-only robot navigation in a neural radiance world. *IEEE Robotics and Automation Letters*, 7(2):4606–4613, 2022.
- [3] Anurag Ajay, Yilun Du, Abhi Gupta, Joshua Tenenbaum, Tommi Jaakkola, and Pulkit Agrawal. Is conditional generative modeling all you need for decision-making? *arXiv preprint arXiv:2211.15657*, 2022.
- [4] Brenna D Argall, Sonia Chernova, Manuela Veloso, and Brett Browning. A survey of robot learning from demonstration. *Robotics and autonomous systems*, 57(5):469–483, 2009.
- [5] Yogesh Balaji, Seungjun Nah, Xun Huang, Arash Vahdat, Jiaming Song, Karsten Kreis, Miika Aittala, Timo Aila, Samuli Laine, Bryan Catanzaro, et al. ediffi: Text-to-image diffusion models with an ensemble of expert denoisers. *arXiv preprint arXiv:2211.01324*, 2022.
- [6] Kevin Black, Mitsuhiko Nakamoto, Pranav Atreya, Homer Walke, Chelsea Finn, Aviral Kumar, and Sergey Levine. Zero-shot robotic manipulation with pre-trained image-editing diffusion models. *arXiv preprint arXiv:2310.10639*, 2023.
- [7] Valts Blukis, Taeyeop Lee, Jonathan Tremblay, Bowen Wen, In So Kweon, Kuk-Jin Yoon, Dieter Fox, and Stan Birchfield. Neural fields for robotic object manipulation from a single image. *arXiv preprint arXiv:2210.12126*, 2022.
- [8] Ang Cao and Justin Johnson. Hexplane: A fast representation for dynamic scenes. In *Proceedings of the IEEE/CVF Conference on Computer Vision and Pattern Recognition*, pages 130–141, 2023.
- [9] Matthew Chang, Aditya Prakash, and Saurabh Gupta. Look ma, no hands! agent-environment factorization of egocentric videos. In *Advances in Neural Information Processing Systems*, 2023.
- [10] Chang Chen, Fei Deng, Kenji Kawaguchi, Caglar Gulcehre, and Sungjin Ahn. Simple hierarchical planning with diffusion. *arXiv preprint arXiv:2401.02644*, 2024.
- [11] Lili Chen, Shikhar Bahl, and Deepak Pathak. Playfusion: Skill acquisition via diffusion from language-annotated play. In *Conference on Robot Learning*, pages 2012–2029. PMLR, 2023.
- [12] Zoey Chen, Sho Kiami, Abhishek Gupta, and Vikash Kumar. Genau: Retargeting behaviors to unseen situations via generative augmentation. *arXiv preprint arXiv:2302.06671*, 2023.
- [13] Cheng Chi, Siyuan Feng, Yilun Du, Zhenjia Xu, Eric Cousineau, Benjamin Burchfiel, and Shuran Song. Diffusion policy: Visuomotor policy learning via action diffusion. *arXiv preprint arXiv:2303.04137*, 2023.
- [14] Cheng Chi, Siyuan Feng, Yilun Du, Zhenjia Xu, Eric Cousineau, Benjamin Burchfiel, and Shuran Song. Diffusion policy: Visuomotor policy learning via action diffusion. In *Proceedings of Robotics: Science and Systems (RSS)*, 2023.
- [15] Patrick Esser, Robin Rombach, and Björn Ommer. Taming transformers for high-resolution image synthesis. *arXiv*, 2020.
- [16] Peter Florence, Lucas Manuelli, and Russ Tedrake. Self-supervised correspondence in visuomotor policy learning. *IEEE Robotics and Automation Letters*, 5(2):492–499, 2019.
- [17] Alessandro Giusti, Jérôme Guzzi, Dan C. Cireşan, Fang-Lin He, Juan P. Rodríguez, Flavio Fontana, Matthias Faessler, Christian Forster, Jürgen Schmidhuber, Gianni Di Caro, Davide Scaramuzza, and Luca M. Gambardella. A machine learning approach to visual perception of forest trails for mobile robots. *IEEE Robotics and Automation Letters*, 1(2):661–667, 2016. doi: 10.1109/LRA.2015.2509024.
- [18] Ian Goodfellow, Jean Pouget-Abadie, Mehdi Mirza, Bing Xu, David Warde-Farley, Sherjil Ozair, Aaron Courville, and Yoshua Bengio. Generative adversarial nets. *Advances in neural information processing systems*, 27, 2014.
- [19] Jiatao Gu, Alex Trevithick, Kai-En Lin, Joshua M Susskind, Christian Theobalt, Lingjie Liu, and Ravi Ramamoorthi. Nerfdiff: Single-image view synthesis with nerf-guided distillation from 3d-aware diffusion. In *International Conference on Machine Learning*, pages 11808–11826. PMLR, 2023.
- [20] Shuyang Gu, Dong Chen, Jianmin Bao, Fang Wen, Bo Zhang, Dongdong Chen, Lu Yuan, and Baining Guo. Vector quantized diffusion model for text-to-image synthesis. In *Proceedings of the IEEE/CVF Conference on Computer Vision and Pattern Recognition*, pages 10696–10706, 2022.
- [21] Richard Hartley and Andrew Zisserman. *Multiple view geometry in computer vision*. Cambridge university press, 2003.
- [22] Kaiming He, Xiangyu Zhang, Shaoqing Ren, and Jian

- Sun. Deep residual learning for image recognition. In *Proceedings of the IEEE Conference on Computer Vision and Pattern Recognition (CVPR)*, 2016.
- [23] Shashank Hegde, Sumeet Batra, KR Zentner, and Gaurav S Sukhatme. Generating behaviorally diverse policies with latent diffusion models. *arXiv preprint arXiv:2305.18738*, 2023.
- [24] Jonathan Ho, Ajay Jain, and Pieter Abbeel. Denoising diffusion probabilistic models. *Advances in Neural Information Processing Systems*, 33:6840–6851, 2020.
- [25] Ahmed Hussein, Mohamed Medhat Gaber, Eyad Elyan, and Chrisina Jayne. Imitation learning: A survey of learning methods. *ACM Computing Surveys (CSUR)*, 50(2):1–35, 2017.
- [26] Dongyoon Hwang, Minhoo Park, and Jiyoung Lee. Sample generations for reinforcement learning via diffusion models. 2023.
- [27] Phillip Isola, Jun-Yan Zhu, Tinghui Zhou, and Alexei A Efros. Image-to-image translation with conditional adversarial networks. In *Proceedings of the IEEE conference on computer vision and pattern recognition*, pages 1125–1134, 2017.
- [28] Eric Jang, Alex Irpan, Mohi Khansari, Daniel Kappler, Frederik Ebert, Corey Lynch, Sergey Levine, and Chelsea Finn. Bc-z: Zero-shot task generalization with robotic imitation learning. In *Conference on Robot Learning*, pages 991–1002. PMLR, 2022.
- [29] Michael Janner, Yilun Du, Joshua B Tenenbaum, and Sergey Levine. Planning with diffusion for flexible behavior synthesis. *arXiv preprint arXiv:2205.09991*, 2022.
- [30] Ivan Kapelyukh, Vitalis Vosylius, and Edward Johns. Dall-e-bot: Introducing web-scale diffusion models to robotics. *IEEE Robotics and Automation Letters*, 2023.
- [31] Liyiming Ke, Jingqiang Wang, Tapomayukh Bhattacharjee, Byron Boots, and Siddhartha Srinivasa. Grasping with chopsticks: Combating covariate shift in model-free imitation learning for fine manipulation. In *2021 IEEE International Conference on Robotics and Automation (ICRA)*, pages 6185–6191. IEEE, 2021.
- [32] Liyiming Ke, Yunchu Zhang, Abhay Deshpande, Siddhartha Srinivasa, and Abhishek Gupta. Ccil: Continuity-based data augmentation for corrective imitation learning. *arXiv preprint arXiv:2310.12972*, 2023.
- [33] Alex Krizhevsky, Ilya Sutskever, and Geoffrey E. Hinton. Imagenet classification with deep convolutional neural networks. In *Advances in Neural Information Processing Systems (NeurIPS)*, 2012.
- [34] Jeong-gi Kwak, Erqun Dong, Yuhe Jin, Hanseok Ko, Shweta Mahajan, and Kwang Moo Yi. Vivid-1-to-3: Novel view synthesis with video diffusion models. *arXiv preprint arXiv:2312.01305*, 2023.
- [35] Michael Laskey, Sam Staszak, Wesley Yu-Shu Hsieh, Jeffrey Mahler, Florian T Pokorny, Anca D Dragan, and Ken Goldberg. Shiv: Reducing supervisor burden in dagger using support vectors for efficient learning from demonstrations in high dimensional state spaces. In *2016 IEEE International Conference on Robotics and Automation (ICRA)*, pages 462–469. IEEE, 2016.
- [36] Michael Laskey, Jonathan Lee, Roy Fox, Anca Dragan, and Ken Goldberg. Dart: Noise injection for robust imitation learning. In *Conference on robot learning*, pages 143–156. PMLR, 2017.
- [37] Wenhao Li, Xiangfeng Wang, Bo Jin, and Hongyuan Zha. Hierarchical diffusion for offline decision making. In *International Conference on Machine Learning*, pages 20035–20064. PMLR, 2023.
- [38] Xiang Li, Varun Belagali, Jinghuan Shang, and Michael S Ryo. Crossway diffusion: Improving diffusion-based visuomotor policy via self-supervised learning. *arXiv preprint arXiv:2307.01849*, 2023.
- [39] Yunzhu Li, Shuang Li, Vincent Sitzmann, Pulkit Agrawal, and Antonio Torralba. 3d neural scene representations for visuomotor control. In *Conference on Robot Learning*, pages 112–123. PMLR, 2022.
- [40] Zhixuan Liang, Yao Mu, Mingyu Ding, Fei Ni, Masayoshi Tomizuka, and Ping Luo. Adaptdiffuser: Diffusion models as adaptive self-evolving planners. *arXiv preprint arXiv:2302.01877*, 2023.
- [41] Zhixuan Liang, Yao Mu, Hengbo Ma, Masayoshi Tomizuka, Mingyu Ding, and Ping Luo. Skilldiffuser: Interpretable hierarchical planning via skill abstractions in diffusion-based task execution. *arXiv preprint arXiv:2312.11598*, 2023.
- [42] Ruoshi Liu, Rundi Wu, Basile Van Hoorick, Pavel Tokmakov, Sergey Zakharov, and Carl Vondrick. Zero-1-to-3: Zero-shot one image to 3d object. In *Proceedings of the IEEE/CVF International Conference on Computer Vision*, pages 9298–9309, 2023.
- [43] Cong Lu, Philip J Ball, and Jack Parker-Holder. Synthetic experience replay. *arXiv preprint arXiv:2303.06614*, 2023.
- [44] Andreas Lugmayr, Martin Danelljan, Andres Romero, Fisher Yu, Radu Timofte, and Luc Van Gool. Repaint: Inpainting using denoising diffusion probabilistic models. In *Proceedings of the IEEE/CVF Conference on Computer Vision and Pattern Recognition*, pages 11461–11471, 2022.
- [45] Corey Lynch, Mohi Khansari, Ted Xiao, Vikash Kumar, Jonathan Tompson, Sergey Levine, and Pierre Sermanet. Learning latent plans from play. In *Conference on robot learning*, pages 1113–1132. PMLR, 2020.
- [46] Zhao Mandi, Homanga Bharadhwaj, Vincent Moens, Shuran Song, Aravind Rajeswaran, and Vikash Kumar. Cacti: A framework for scalable multi-task multi-scene visual imitation learning. *arXiv preprint arXiv:2212.05711*, 2022.
- [47] Chenlin Meng, Yutong He, Yang Song, Jiaming Song, Jiajun Wu, Jun-Yan Zhu, and Stefano Ermon. Sedit: Guided image synthesis and editing with stochastic differential equations. *arXiv preprint arXiv:2108.01073*, 2021.

- [48] Ben Mildenhall, Pratul P Srinivasan, Matthew Tancik, Jonathan T Barron, Ravi Ramamoorthi, and Ren Ng. Nerf: Representing scenes as neural radiance fields for view synthesis. *Communications of the ACM*, 65(1):99–106, 2021.
- [49] Jyothish Pari, Nur Muhammad, Sridhar Pandian Arunachalam, and Lerrel Pinto. The surprising effectiveness of representation learning for visual imitation. *arXiv preprint arXiv:2112.01511*, 2021.
- [50] Dean A Pomerleau. Alvin: An autonomous land vehicle in a neural network. *Advances in neural information processing systems*, 1, 1988.
- [51] Dean A Pomerleau. Efficient training of artificial neural networks for autonomous navigation. *Neural computation*, 3(1):88–97, 1991.
- [52] Aditya Ramesh, Prafulla Dhariwal, Alex Nichol, Casey Chu, and Mark Chen. Hierarchical text-conditional image generation with clip latents. *arXiv preprint arXiv:2204.06125*, 1(2):3, 2022.
- [53] Robin Rombach, Andreas Blattmann, Dominik Lorenz, Patrick Esser, and Björn Ommer. High-resolution image synthesis with latent diffusion models. 2022 IEEE In *CVF Conference on Computer Vision and Pattern Recognition (CVPR)*, pages 10674–10685, 2021.
- [54] Robin Rombach, Andreas Blattmann, Dominik Lorenz, Patrick Esser, and Björn Ommer. High-resolution image synthesis with latent diffusion models. In *CVPR*, pages 10684–10695, 2022.
- [55] Olaf Ronneberger, Philipp Fischer, and Thomas Brox. U-net: Convolutional networks for biomedical image segmentation. In *MICCAI*, pages 234–241. Springer, 2015.
- [56] Stéphane Ross, Geoffrey Gordon, and Drew Bagnell. A reduction of imitation learning and structured prediction to no-regret online learning. In *Proceedings of the fourteenth international conference on artificial intelligence and statistics*, pages 627–635, 2011.
- [57] Chitwan Saharia, William Chan, Saurabh Saxena, Lala Li, Jay Whang, Emily L Denton, Kamyar Ghasemipour, Raphael Gontijo Lopes, Burcu Karagol Ayan, Tim Salimans, et al. Photorealistic text-to-image diffusion models with deep language understanding. *Advances in Neural Information Processing Systems*, 35:36479–36494, 2022.
- [58] Stefan Schaal. Learning from demonstration. *Advances in neural information processing systems*, 9, 1996.
- [59] Johannes Lutz Schönberger and Jan-Michael Frahm. Structure-from-motion revisited. In *Conference on Computer Vision and Pattern Recognition (CVPR)*, 2016.
- [60] Johannes Lutz Schönberger, Enliang Zheng, Marc Pollefeys, and Jan-Michael Frahm. Pixelwise view selection for unstructured multi-view stereo. In *European Conference on Computer Vision (ECCV)*, 2016.
- [61] Nur Muhammad Shafiullah, Zichen Cui, Ariuntuya Arty Altanzaya, and Lerrel Pinto. Behavior transformers: Cloning k modes with one stone. *Advances in neural information processing systems*, 35:22955–22968, 2022.
- [62] Nur Muhammad Mahi Shafiullah, Anant Rai, Haritheja Etukuru, Yiqian Liu, Ishan Misra, Soumith Chintala, and Lerrel Pinto. On bringing robots home. *arXiv preprint arXiv:2311.16098*, 2023.
- [63] Jascha Sohl-Dickstein, Eric Weiss, Niru Maheswaranathan, and Surya Ganguli. Deep unsupervised learning using nonequilibrium thermodynamics. In *International conference on machine learning*, pages 2256–2265. PMLR, 2015.
- [64] Shuran Song, Andy Zeng, Johnny Lee, and Thomas Funkhouser. Grasping in the wild: Learning 6dof closed-loop grasping from low-cost demonstrations. *Robotics and Automation Letters*, 2020.
- [65] Yang Song and Stefano Ermon. Generative modeling by estimating gradients of the data distribution. *Advances in neural information processing systems*, 32, 2019.
- [66] Shih-Yang Su, Frank Yu, Michael Zollhöfer, and Helge Rhodin. A-nerf: Articulated neural radiance fields for learning human shape, appearance, and pose. *Advances in Neural Information Processing Systems*, 34:12278–12291, 2021.
- [67] Matthew Tancik, Ethan Weber, Evonne Ng, Ruilong Li, Brent Yi, Terrance Wang, Alexander Kristoffersen, Jake Austin, Kamyar Salahi, Abhik Ahuja, et al. Nerfstudio: A modular framework for neural radiance field development. In *ACM SIGGRAPH 2023 Conference Proceedings*, pages 1–12, 2023.
- [68] Sebastian Thrun. Probabilistic robotics. *Communications of the ACM*, 45(3):52–57, 2002.
- [69] Hung-Yu Tseng, Qinbo Li, Changil Kim, Suhub Alsisan, Jia-Bin Huang, and Johannes Kopf. Consistent view synthesis with pose-guided diffusion models. In *Proceedings of the IEEE/CVF Conference on Computer Vision and Pattern Recognition*, pages 16773–16783, 2023.
- [70] Yixuan Wang, Zhuoran Li, Mingtong Zhang, Katherine Driggs-Campbell, Jiajun Wu, Li Fei-Fei, and Yunzhu Li. d^3 fields: Dynamic 3d descriptor fields for zero-shot generalizable robotic manipulation. *arXiv preprint arXiv:2309.16118*, 2023.
- [71] Zhendong Wang, Jonathan J Hunt, and Mingyuan Zhou. Diffusion policies as an expressive policy class for offline reinforcement learning. *arXiv preprint arXiv:2208.06193*, 2022.
- [72] Daniel Watson, William Chan, Ricardo Martin-Brualla, Jonathan Ho, Andrea Tagliasacchi, and Mohammad Norouzi. Novel view synthesis with diffusion models. *arXiv preprint arXiv:2210.04628*, 2022.
- [73] Zhou Xian, Nikolaos Gkanatsios, Theophile Gervet, Tsung-Wei Ke, and Katerina Fragkiadaki. Chaineddiffuser: Unifying trajectory diffusion and keypose prediction for robotic manipulation. In *Conference on Robot Learning*, pages 2323–2339. PMLR, 2023.
- [74] Tete Xiao, Ilija Radosavovic, Trevor Darrell, and Jitendra Malik. Masked visual pre-training for motor control. *arXiv preprint arXiv:2203.06173*, 2022.
- [75] Jiawei Yang, Marco Pavone, and Yue Wang. Freenerf:

- Improving few-shot neural rendering with free frequency regularization. In *Proceedings of the IEEE/CVF Conference on Computer Vision and Pattern Recognition*, pages 8254–8263, 2023.
- [76] Yufei Ye, Xueting Li, Abhinav Gupta, Shalini De Mello, Stan Birchfield, Jiaming Song, Shubham Tulsiani, and Sifei Liu. Affordance diffusion: Synthesizing hand-object interactions. In *Proceedings of the IEEE/CVF Conference on Computer Vision and Pattern Recognition*, pages 22479–22489, 2023.
- [77] Sarah Young, Dhiraj Gandhi, Shubham Tulsiani, Abhinav Gupta, Pieter Abbeel, and Lerrel Pinto. Visual imitation made easy. In *Conference on Robot Learning*, pages 1992–2005. PMLR, 2021.
- [78] Sarah Young, Jyothish Pari, Pieter Abbeel, and Lerrel Pinto. Playful interactions for representation learning. In *2022 IEEE/RSJ International Conference on Intelligent Robots and Systems (IROS)*, pages 992–999. IEEE, 2022.
- [79] Alex Yu, Vickie Ye, Matthew Tancik, and Angjoo Kanazawa. pixelnerf: Neural radiance fields from one or few images. In *Proceedings of the IEEE/CVF Conference on Computer Vision and Pattern Recognition*, pages 4578–4587, 2021.
- [80] Jason J Yu, Fereshteh Forghani, Konstantinos G Derpanis, and Marcus A Brubaker. Long-term photometric consistent novel view synthesis with diffusion models. *arXiv preprint arXiv:2304.10700*, 2023.
- [81] Tianhe Yu, Ted Xiao, Austin Stone, Jonathan Tompson, Anthony Brohan, Su Wang, Jaspiar Singh, Clayton Tan, Jodilyn Peralta, Brian Ichter, et al. Scaling robot learning with semantically imagined experience. *arXiv preprint arXiv:2302.11550*, 2023.
- [82] Lvmin Zhang, Anyi Rao, and Maneesh Agrawala. Adding conditional control to text-to-image diffusion models. In *Proceedings of the IEEE/CVF International Conference on Computer Vision*, pages 3836–3847, 2023.
- [83] Tianhao Zhang, Zoe McCarthy, Owen Jow, Dennis Lee, Xi Chen, Ken Goldberg, and Pieter Abbeel. Deep imitation learning for complex manipulation tasks from virtual reality teleoperation. In *2018 IEEE International Conference on Robotics and Automation (ICRA)*, pages 5628–5635. IEEE, 2018.
- [84] Tony Z Zhao, Vikash Kumar, Sergey Levine, and Chelsea Finn. Learning fine-grained bimanual manipulation with low-cost hardware. *arXiv preprint arXiv:2304.13705*, 2023.
- [85] Allan Zhou, Moo Jin Kim, Lirui Wang, Pete Florence, and Chelsea Finn. Nerf in the palm of your hand: Corrective augmentation for robotics via novel-view synthesis. In *Proceedings of the IEEE/CVF Conference on Computer Vision and Pattern Recognition*, pages 17907–17917, 2023.
- [86] Yuke Zhu, Ziyu Wang, Josh Merel, Andrei Rusu, Tom Erez, Serkan Cabi, Saran Tunyasuvunakool, János Kramár, Raia Hadsell, Nando de Freitas, et al. Reinforcement and imitation learning for diverse visuomotor skills. *arXiv preprint arXiv:1802.09564*, 2018.